WOOD MATERIAL SCIENCE & ENGINEERING
https://doi.org/10.1080/17480272.2026.2674759

Taylor & Francis
by informa

ORIGINAL ARTICLE

Valorization of downed timber into wood fibers for polypropylene composites: effects of tree maturity and environmental exposure duration

Ke Zhan[a,b], Courtney Higgins[b], Mi Li[c], Mathew Smidt[d], Thomas Elder[b], Wei Gao[a] and Yucheng Peng[b]

[a]College of Materials and Chemical Engineering, Southwest Forestry University, Kunming, People's Republic of China; [b]College of Forestry, Wildlife and Environment, Auburn University, Auburn, AL, USA; [c]Center for Renewable Carbon, School of Natural Resources, University of Tennessee, Knoxville, TN, USA; [d]Southern Research Station, USDA-Forest Service, Auburn, AL, USA

ABSTRACT

Hurricanes generate a large volume of downed timber in the southeastern United States each year. Utilizing this timber as a source of wood fibers (WFs) for reinforcing polypropylene (PP) could help mitigate landowners' economic losses. This study investigated the effects of tree age and environmental exposure on the sizes, morphologies, and surface properties of WFs from downed timber, as well as the mechanical and rheological behaviors of PP composites reinforced with these WFs at different loading levels. Tree age emerged as the dominant factor affecting strength, while loading level played a key role in enhancing stiffness, and exposure duration had a relatively minor influence. The major findings discovered that fibers with high maturity contributed to enhanced mechanical performance, while fibers from older trees, containing high extractive content, were more prone to degradation under extended exposure durations. Overall, all composite exhibited significantly higher tensile, flexural, and impact strengths than neat PP. The rheological study further explored fiber-matrix interactions, providing critical insights into the fiber quality and the processability of the composites. The WFs derived from downed timber harvested within 12 months demonstrate great potential for use as reinforcement in PP.

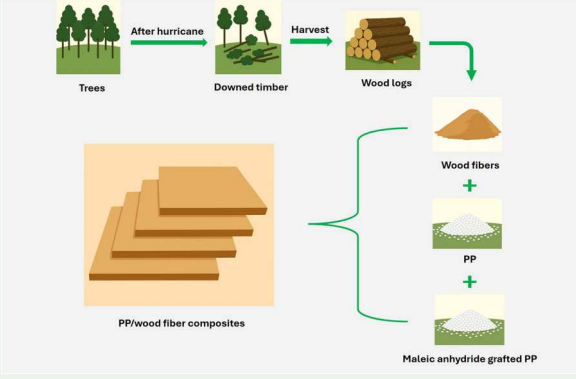

ARTICLE HISTORY
Received 24 November 2025
Revised 27 March 2026
Accepted 7 May 2026

KEYWORDS
Windthrown timber; WPCs; plastics; mechanical properties; rheological properties

Highlights

- Wood fibers produced from downed timber can enhance the mechanical performance of PP, mainly determined by the fiber loading levels.
- The tree maturity and duration of environmental exposure significantly affect the wood fiber properties, resulting in significant differences of the properties of the manufactured composites.
- The composites with wood fibers from the 30-year-old tree showed the greatest Izod impact strengths at all the loading levels and all the different environmental exposure periods.
- Environmental exposure duration showed a greater effect on the performance of composites with wood fibers from the 39-year-old tree than those with fibers from 15- and 30-year-old trees.
- Rheological behaviors of the composites provided insights into the fiber quality after environmental exposure and the interactions between fibers and the polymer matrix.

1. Introduction

As the climate warms, extreme weather events are becoming more frequent and severe, causing substantial impacts across various sectors of human society. In the United States, hurricanes result in billions of dollars in damage and more than one hundred fatalities annually (Moore *et al.* 2015). The

CONTACT Yucheng Peng yzp0027@auburn.edu College of Forestry, Wildlife and Environment, Auburn University, Auburn 36849, AL, USA
Supplemental data for this article can be accessed online at https://doi.org/10.1080/17480272.2026.2674759.

southeastern United States has abundant forest resources and plays a significant role in global timber supply markets (He *et al.* 2016, Guo *et al.* 2023). However, as one of the regions most frequently affected by hurricanes, the southeastern United States experiences extensive damage to its forest land, resulting in a large volume of downed timber each year. For example, Hurricane Katrina in 2005 damaged approximately five million acres of forest land in Mississippi, resulting in an estimated timber loss of 125 million tons, equivalent to about five years of the state's annual harvest (Aladwan 2021). Hurricane Michael in 2018 affected an estimated 2.8 million acres of forest land (Hernandez-Diaz *et al.* 2024). Hurricane Helene in 2024 caused an estimated 0.82 million acres of timber loss, resulting in approximately 214 million dollars in damages to North Carolina forests (Callaghan 2025). Additional forest land damages have also been reported in recent years due to hurricanes such as Nate 2017, Zeta 2020, Ian 2022, and Idalia 2023 (Aladwan 2021, Karasinski *et al.* 2023, Corkran *et al.* 2024). Exploring potential pathways to valorize this downed timber could help minimize the economic losses faced by landowners.

Wood polymer composites (WPCs), comprising wood fibers (WFs) as the dispersed phase and a polymer as the matrix, are widely utilized as structural materials in various engineering applications, including decking, building components, and automotive interior parts (Ayana *et al.* 2024). Among various polymer matrices, polypropylene (PP) is one of the most widely employed thermoplastic matrices in WPC manufacturing (Andrzejewski *et al.* 2024). The incorporation of WFs into the PP matrix helps overcome the limitations of PP's inherent low stiffness and impact resistance, which often lead to inadequate mechanical performance for engineering structural components (Ferdinánd *et al.* 2023). PP-based WPCs have been extensively studied, exhibiting satisfactory mechanical properties with the incorporation of WFs and showing strong potential for large-scale commercialization (Park and Balatinecz 1997, Bledzki and Faruk 2003, Hristov *et al.* 2004, Smith and Wolcott 2006, Pérez *et al.* 2012, Gardner *et al.* 2015, Wang *et al.* 2020, Ferdinánd *et al.* 2023). For example, WFs derived from maple enhanced the tensile strength, thermal stability, dielectric constant, and conductivity of WPCs with PP as the matrix (Ben Hamou *et al.* 2023, Basiji *et al.* 2025a, Basiji *et al.* 2025b). In addition, maple fibers also improved the tensile strength and dimensional stability of WPCs with high-density polyethylene (HDPE) as the matrix (Tazi *et al.* 2014, Tazi *et al.* 2016). These studies demonstrate the potential of WFs for use as a reinforcement in plastics such as PP and HDPE. Using downed timber generated by hurricanes as a resource of WFs for WPC manufacturing could be a sustainable approach to valorize this material. This strategy not only helps meet the increasing demand for WPC raw materials but also opens up new market opportunities for the utilization of downed timber. However, the quality of WFs derived from downed timber, as well as the corresponding performance of the resulting WPCs, needs to be carefully evaluated before commercial application. There are two major factors that play critical roles in determining the quality of the WFs and the properties of the resulting composites.

The first factor is tree maturity. Unlike managed harvesting, timber downed by hurricanes varies widely in tree age, resulting in inconsistencies in fiber quality and composition. For instance, a 15-year-old loblolly pine consists of approximately 85% juvenile wood by volume, whereas a 40-year-old tree contains only about 19% (Zobel and Blair 1976). Juvenile and mature woods exhibit notable differences in chemical components, as the relative amounts of cellulose, hemicellulose, and lignin within the cell wall differ considerably. These variations influence the mechanical properties and processing behavior of WFs (Khodayari *et al.* 2021). Mature wood generally contains a higher cellulose content, whereas juvenile wood has a greater proportion of lignin (Bao *et al.* 2001). Cellulose is a stiff and highly crystalline polymer, and a higher cellulose content endows the WFs with greater tensile strength and stiffness (Ray *et al.* 2021). Lignin, on the other hand, is an inherently brittle polymer; increased lignin content reduces the flexibility and energy absorption capacity of the WFs, resulting in lower toughness in the resulting composites (Ten and Vermerris 2015). Hemicellulose acts as an amorphous binding component between cellulose and lignin, influencing the flexibility, moisture absorption, and interfacial bonding behavior of the WFs (Gunwant 2024). In addition to chemical composition, physical and structural parameters, including fiber length, density, and microfibril angle, also affect the mechanical performance of the WFs. Juvenile wood generally contains a larger proportion of earlywood, lower density, shorter fiber length, and a higher microfibril angle compared with mature wood (Clark *et al.* 2006, Via *et al.* 2007, Lu *et al.* 2021). These characteristics tend to reduce the strength and stiffness of the WFs, consequently having less reinforcing effect on the mechanical performance of the resulting WPCs (Via *et al.* 2009). Moreover, the extractive content also changes with tree age, as older trees develop more heartwood, which contains higher levels of extractives such as tannins and resins than sapwood (Hillis 1971, Pinto *et al.* 2004). These extractives can influence the surface energy and wettability of the WFs, thereby affecting their interactions with the polymer matrix and the compatibilizer.

The second factor is the duration of environmental exposure. Following a hurricane, the overwhelming volume of downed timber often exceeds the available capacity for timely collection due to constraints such as narrow harvesting windows, limited logging equipment, and insufficient labor resources (Aghalari *et al.* 2021). Consequently, a significant portion of the downed timber remains in the field for extended periods, often several weeks or months. During this time, prolonged exposure to moisture, sunlight, temperature fluctuations, and biological activity accelerates the degradation of wood, resulting in changes to the structure, chemistry, and overall quality of the WFs. Fungal decay is the major cause of wood quality degradation, with brown rot, white rot, and soft rot being the commonly reported types, each differing in its mechanism of cell wall decomposition (Schwarze 2007). Brown-rot fungi primarily attack softwoods and are typically active above ground, decomposing cellulose and hemicellulose while leaving lignin largely intact (Broda and Popescu 2019). Most white-rot fungi depolymerize cellulose, hemicellulose, and lignin simultaneously, whereas some selective white-rot fungi preferentially degrade hemicellulose and lignin, leaving much of the crystalline cellulose relatively undegraded (Goodell *et al.* 2020). Soft-rot fungi mainly decompose cellulose

and hemicellulose, with only slight modification of lignin, and are often active under high-moisture conditions where other decay fungi cannot thrive (Martínez *et al.* 2005, Daniel 2014). Mold and stain fungi can affect the appearance of wood and degrade certain extractives, but do not attack the structural components of the wood cell wall (Martínez *et al.* 2005, Gao *et al.* 2024). Hemicellulose is a low-molecular-weight polymer that generally degrades first, followed by the partial degradation of cellulose in the amorphous regions (Schwarze 2007). Lignin is the most resistant component to fungal degradation and typically decomposes at later stages, primarily through oxidative and enzymatic reactions mediated by white-rot fungi (Ten Have and Teunissen 2001, Janusz *et al.* 2017). As degradation progresses with increasing environmental exposure duration, the loss of structural components in the WFs results in changes to their strength, stiffness, and surface energy, all of which ultimately affect the overall performance of the WPCs. During this period, insect and pest activity may further deteriorate wood (Martín and López 2023). Additionally, leaching can cause the loss of non-structural extractives, increasing the wood's susceptibility to fungal decay through repeated wetting and drying cycles associated with weather fluctuations (Kirker *et al.* 2013, Kirker *et al.* 2024). Therefore, the degradation of downed timber is a complex process influenced by multiple factors, including but not limited to site conditions, tree age, soil type, moisture, relative humidity, and temperature.

The objective of this study was to investigate the effects of tree maturity and environmental exposure duration on the properties of WFs produced from downed timbers and on their performance in reinforcing PP. Loblolly pine (*Pinus taeda* L.) trees of different ages (15, 30, and 39 years) were felled and exposed to the environment for varying durations (0, 6, and 12 months) to simulate downed timbers resulting from frequent hurricanes in the southeastern United States. WFs were produced from the downed timbers, and their particle size distribution, morphology, and surface properties were characterized. The mechanical and rheological properties of PP composites reinforced with these WFs were evaluated. This study examined new opportunities for utilizing hurricane-damaged, downed timber to mitigate landowners' economic losses.

2. Materials and methods

2.1. Materials

Commercial grade homopolymer PP pellets (PP1024E) with a density of 900 kg/m^3 and a melt flow index of 13 g/10 min at 230°C/2.16 kg were supplied by ExxonMobil Chemical Company (Baytown, TX, USA). Maleic anhydride grafted PP (MAPP) pellets (Polybond 3200), purchased from ChemPoint Inc. (Bellevue, WA, USA), had a density of 910 kg/m^3, a melt flow index of 115 g/10 min at 190°C/2.16 kg, and a maleic anhydride content between 0.8 wt.% and 1.2 wt.%. WFs with varying maturity levels and environmental exposure periods were produced from downed timbers. MAPP and WFs were dried overnight in a forced-air oven at 105°C to remove moisture before use.

2.2. Production of WFs from downed timbers

Three loblolly pine (*Pinus taeda* L.) trees, aged 15, 30, and 39 years (denoted as L15, L30, and L39), were felled at a stump height of approximately 30 cm on October 22, 2020, at the Solon Dixon Forestry Education Center in Andalusia, South Alabama, United States. Because one tree was used per age group in this study, 'tree age' reflects differences among these representative trees and should be interpreted accordingly. Each tree was left on the forest floor and exposed to natural environmental conditions for 0, 6, and 12 months (denoted as 0M, 6M, and 12M) to simulate downed timbers with varying exposure durations. The felled trees were placed directly on the forest floor with full ground contact, under natural canopy cover and local climatic conditions (temperature, precipitation, and humidity) at one field site, although some residual uncontrolled variability (e.g. minor differences in moisture, microbial activity, and shading) may still exist and influence the results. Following the exposure periods, log samples with lengths of 15-30 cm were cut from the bottom of each tree and stored at −20°C in a laboratory freezer until use.

The log samples were processed to produce WFs through the following steps: (1) The log samples were debarked and sectioned into discs using a Farm Boss chainsaw. (2) These discs were subsequently reduced into wood blocks with maximum dimensions of 254 × 127 × 76 mm using a table saw and a band saw, making them suitable for feeding into a chipper. (3) Chipping was performed using a 12.7 × 8.9 cm 457cc Brush Master chipper shredder CH11 (Maple Grove, MN, USA), yielding wood chips with an approximate dimension of 25.4 × 12.7 × 12.7 mm. (4) The wood chips were then milled using a Thomas Wiley mill (Model No. 3375-E20, Thomas Scientific, Swedesboro, NJ, USA) equipped with a 2 mm screen. (5) The resulting WFs were further refined using a Retsch cutting mill SM300 (Retsch, Newtown, PA, USA) equipped with a 40-mesh screen, operating at a blade rotation speed of 1500 rpm. The final WFs were stored in Ziploc bags for subsequent use. The WFs were designated using a combination of tree age and exposure period. For example, "L15-6M" represents the WFs produced from 15-year-old trees that have been exposed to the environment for 6 months. This naming format (including 'M' for months) is used consistently throughout the manuscript.

2.3. Manufacture of PP/WF composites

PP/WF composites were prepared in an internal mixer (Model 2128, C.W. Brabender Instruments, Inc., Hackensack, NJ, US), equipped with two counter-rotating roller blades. The mixing temperature and mixing speed were set as 180°C and 60 rpm, respectively. The MAPP content was maintained at 5 wt.% across all composites, while the WF loading levels were 30, 40, and 50 wt.% for each combination of tree age and exposure period. Maintaining MAPP at 5 wt% across all formulations changes the effective MAPP/WF ratio with loading level; this constraint is noted when interpreting loading-dependent trends. PP pellets were fed into the mixer chamber and mixed for 3 min. Afterward, MAPP pellets were added and

mixed for an additional 2 min. WFs were then gradually added to the mixer within 1 min and allowed to mix for an additional 5 min. Afterward, the composites were scraped off the mixer while still in a molten state and allowed to solidify at room temperature.

The solidified composites were then ground into particles using a low-speed granulator (Model SG-2042NH, Shini Plastic Technologies, Inc., Willoughby, OH, US) equipped with a 3 mm sieve. The particles were dried in an oven overnight at 105°C to remove moisture before injection molding. A benchtop injection molding machine (Proto-Ject 150 HP, Manning Innovations, Inc., Halls, TN, US) was employed to produce test specimens using customized aluminum molds. Specimens for mechanical testing were injection-molded to specified dimensions in compliance with the relevant ASTM standards, while 1.5 mm thick sheets were produced using a specific mold for rheological measurements. The injection molding was conducted at a temperature of 200°C and a pressure of 44 MPa. All specimens were stored in Ziploc bags to prevent moisture intrusion prior to characterization. The PP/WF composites were designated using a combination of tree age, exposure period, and WF loading level. For example, "L15-6M-30%" represents a composite made from WFs generated from 15-year-old trees exposed to the environment for 6 months at the loading level of 30 wt.%.

2.4. Characterizations

2.4.1. Particle size analysis

The particle size distribution of WFs was determined through sieve analysis using a mechanical sieve shaker (Humboldt Model H-4330, Elgin, IL, USA), equipped with brass sieves (Advantech Manufacturing, Inc., New Berlin, WI, USA) measuring 20 cm in diameter and 5 cm in depth. The sieves, corresponding to US standard mesh numbers 140 (106 µm), 100 (150 µm), 80 (180 µm), 60 (250 µm), and 40 (425 µm), were stacked in descending order of mesh size from 425 µm to 106 µm. Approximately 25 g of sample was placed on the top sieve with a mesh size of 425 µm, and a bottom pan was positioned beneath the 106 µm sieve to collect passing WF particles. The shaker was operated for 20 min at a motor speed of 1725 rpm. The mass of WF particles retained between consecutive sieves was weighed to represent the size fraction of fibers within specific size ranges. Each sample was sieved three times to ensure statistical reliability. A limitation of sieve-based particle analysis is that it does not characterize fiber aspect ratio or length distribution, both of which could influence composite reinforcement.

2.4.2. Inverse gas chromatography

The surface area and surface energy of the WFs were analyzed using an inverse gas chromatography (IGC) surface energy analyzer equipped with a flame ionization detector (Surface Measurements Systems, Ltd., Alperton, UK), following a published procedure (Zhang *et al.* 2023). Before the measurement, the WFs were dried under vacuum at room temperature for approximately 24 h. About 45 to 50 mg of the dried sample was accurately weighed and quantitatively packed into individual silanized glass columns (300 mm in length, 4 mm inner diameter) using a column packing accessory. The Brunauer–Emmett–Teller (BET) specific surface area of the WFs was determined by calculating the isotherm of nonane with a pressure ratio (P/P_0) ranging from 0.05 to 0.35. The dispersive (γ^d) and specific acid–base (γ^{ab}) surface energies were assessed over a fractional surface coverage of 0.01 to 0.4 n/nm by introducing non-polar n-alkanes (octane, nonane, and decane) and polar probe molecules (acetone, ethanol, acetonitrile, ethyl acetate, and dichloromethane). Data was analyzed using advanced surface energy analysis software (Advance Version 1.4.2.0) and reported as the average of two replicates. The IGC data with standard deviations is provided in Table S36 in the Supplementary Materials.

2.4.3. Mechanical tests

Tensile testing was conducted at room temperature and following ASTM D638 (Type IV) using a Mark-10 universal testing machine (Model F1505, Copiague, NY, US) equipped with a 1000 N load cell and a resolution of 0.5 N. Strains were measured with an Epsilon extensometer (Model SN E109112, Jackson, WY, US) as the samples were stretched. The testing speed and initial strain rate were set to 5 mm/min and 0.1 min^{-1}, respectively. Average values for tensile strength at yield, tensile modulus of elasticity (MOE), and tensile elongation at yield were calculated from at least seven replicates and reported with standard deviations as error bars. Flexural testing was conducted in accordance with ASTM D790 using a Mark-10 universal testing machine (Model ESM750S, Copiague, NY, USA) equipped with a 500 N load cell and a resolution of 0.2 N. A support span of 50 mm and a crosshead motion speed of 1.34 mm/min were used. Average values for flexural strength at yield and flexural MOE were obtained from at least five replicates and reported along with their standard deviations. Yield was defined as first local maximum stress, and the same criterion was applied consistently across all formulations. Notched Izod impact strength was measured according to ASTM D256 using an XJUD digital impact tester (Deli Group Co. Ltd., Ningbo, China) configured in Izod mode (pendulum energy 1 J; notch geometry per ASTM D256). The average values and standard deviations were calculated from ten replicates and reported. All mechanical tests were performed at room temperature.

A three-way analysis of variance (ANOVA) was conducted on the mechanical testing results using Origin 2025 software at a significance level of $\alpha = 0.05$ to evaluate the interactions among three factors: WF loading level, tree age, and exposure period. To further analyze the effects of each factor, a Tukey's Honestly Significant Difference (HSD) post-hoc test was applied following the ANOVA.

2.4.4. Scanning electron microscopy

The WFs and the fractured surfaces of the PP/WF composites from impact testing specimens were examined using scanning electron microscope (SEM, EVO 50, Zeiss, Oberkochen, Germany), operated at an accelerating voltage of 20 kV. The WFs were evenly spread onto conductive tapes affixed to the sample-supporting stubs, while the fractured surfaces were also mounted on the conductive tapes. The stubs with specimens were sputter-coated with gold for 2 min using a sputter

coater (Q150R, Electron Microscopy Sciences, Hatfield, PA, USA) to enhance conductivity.

2.4.5. Rheological measurements

Rheological behaviors of the composites not only help in understanding the interaction between different phases within the composite but also help understand the processing potential of the composite. For example, in Erchiqui's work, the thermoformability potential of WF-reinforced composites was studied with the assistance of computer analysis (Erchiqui *et al.* 2008, Erchiqui *et al.* 2009, Sukiman *et al.* 2020). In this study, rheological properties of PP/WF composites were investigated using a rheometer (HAAKE MARS 60, Thermo Fisher Scientific, Germany) equipped with a parallel plate geometry (25 mm diameter and 1.3 mm gap). Circular specimens with a diameter of 22 mm were prepared by punching them out of 1.5 mm thick sheets produced by injection-molding using a gasket punch (General Tools, Cincinnati, OH, USA). All rheological tests were conducted at 200°C. The linear viscoelastic region (LVR) was identified through strain sweeps at a frequency of 10 rad/s. A strain of 0.1% was selected for the oscillatory frequency sweep tests performed over an angular frequency range of 0.1 to 600 rad/s. All results were averaged over three replicates and presented with error bars representing standard deviations.

3. Results and discussion

3.1. WF particle size distributions, morphologies, and surface properties

The particle size distributions of the WFs produced from downed timbers are presented in Table 1. Prior to environmental exposure, the particle size distributions of WFs from 15-, 30-, and 39-year-old trees were similar, except for a higher proportion of WFs larger than 425 µm from the 15-year-old tree. The total proportion of WFs larger than 250 µm was comparable across the three tree ages, measuring 58.3%, 54.6%, and 56.5%, respectively. After environmental exposure, the total proportion of WFs larger than 250 µm decreased in the 15-year-old tree compared to the unexposed sample. However, the proportion of WFs within the 250–425 µm range remained largely unchanged in the L15-12M sample. Meanwhile, the proportion of finer WFs (< 250 µm) increased after both 6- and 12-month exposure durations. A similar trend was observed in the 30- and 39-year-old trees, where the proportion of WFs smaller than 250 µm increased, while those larger than 250 µm decreased markedly.

Overall, the tree age had a minimal impact on particle size distribution, whereas the environmental exposure promoted fiber fragmentation and increased the proportion of fine WFs, although the effect of exposure duration (6 versus 12 months) was inconsistent. The observed reduction in particle size after exposure is likely attributed to the degradation of lignin and hemicellulose caused by UV radiation, moisture fluctuations, temperature changes, and microbial activity. Slight variations in the location of downed timber may have significantly influenced these degradation processes, leading to inconsistent impacts of exposure duration. Moreover, no distinct difference in specific surface area (Table 1) was observed among all WFs, except for a relatively low value in the L15-0M WFs. This can be attributed to the higher percentage of WFs greater than 425 µm, as larger fibers have a lower surface area relative to their volume compared to smaller fibers.

The morphologies of the WFs are shown in Figure 1, with the original SEM images provided in Figures S4 to S21. Large variations in particle size were observed across all WFs, ranging from short debris less than 100 µm to long fibers greater than 400 µm, consistent with the measured results in Table 1. All WFs exhibited similar shapes with a relatively high aspect ratio, which is favorable for serving as reinforcement in polymer composites. High aspect ratio fibers tend to align in the flow direction during polymer composite processing, such as extrusion and injection molding, resulting in enhanced stress transfer capacity (Liu *et al.* 2024).

Rough surfaces with distinct wood cell walls were noticeable in the WFs from the 15-year-old and 30-year-old trees. In contrast, the WFs from the 39-year-old tree appeared smoother, particularly in the L39-0M fibers. This is likely due to the higher proportion of extractives, such as resins, waxes, phenolic compounds, and tannins, in the older tree (Miranda and Pereira 2002, Mohammadi *et al.* 2011, Sivan *et al.* 2023). The WFs were subjected to milling during production, where the heat generated by friction and shear forces softened lignin and partial extractives, causing them to migrate to the fiber surfaces. This process filled surface voids and formed a thin layer around the cellulose fibers, consequently reducing surface roughness. The smoother fiber surface may weaken the fiber-matrix adhesion in polymer composites, reducing stress transfer efficiency and ultimately compromising mechanical strength.

Figure 2 presents the dispersive and acid–base components of the surface energy of the WFs. Before environmental

Table 1. Particle size distributions and specific surface areas of the WFs.

Sample name	Particle size distributions (%)						Specific surface area (m^2/g)
	< 106 µm	106–150 µm	150–180 µm	180–250 µm	250–425 µm	> 425 µm	
L15-0M	16.5 ± 0.2	6.5 ± 0.4	4.8 ± 0.2	14.0 ± 0.2	47.8 ± 0.4	10.4 ± 0.2	2.9 ± 0.2
L15-6M	21.8 ± 1.5	11.9 ± 0.4	10.4 ± 1.3	19.6 ± 0.7	32.3 ± 0.7	4.1 ± 0.1	3.6 ± 0.4
L15-12M	19.1 ± 0.3	8.2 ± 0.2	5.9 ± 0.2	16.1 ± 0.4	48.7 ± 0.1	2.0 ± 0.1	4.3 ± 0.2
L30-0M	18.4 ± 0.2	5.9 ± 2.5	4.7 ± 0.3	16.5 ± 0.7	53.4 ± 1.3	1.2 ± 0.1	4.3 ± 0.2
L30-6M	26.3 ± 0.3	13.8 ± 0.5	8.6 ± 0.2	17.4 ± 0.3	31.2 ± 0.4	2.7 ± 0.2	3.6 ± 0.1
L30-12M	21.0 ± 0.1	12.0 ± 0.2	10.6 ± 0.3	22.1 ± 0.6	31.7 ± 0.5	2.6 ± 0.2	3.9 ± 0.4
L39-0M	13.0 ± 0.1	7.6 ± 0.4	4.7 ± 0.2	18.2 ± 0.6	55.3 ± 0.1	1.2 ± 0.1	4.1 ± 0.2
L39-6M	20.8 ± 0.3	9.2 ± 0.2	6.5 ± 0.1	17.5 ± 0.2	38.8 ± 0.3	7.3 ± 0.1	3.4 ± 0.1
L39-12M	23.6 ± 0.4	8.5 ± 0.2	6.4 ± 0.4	16.7 ± 0.2	42.8 ± 0.3	2.0 ± 0.1	3.6 ± 0.6

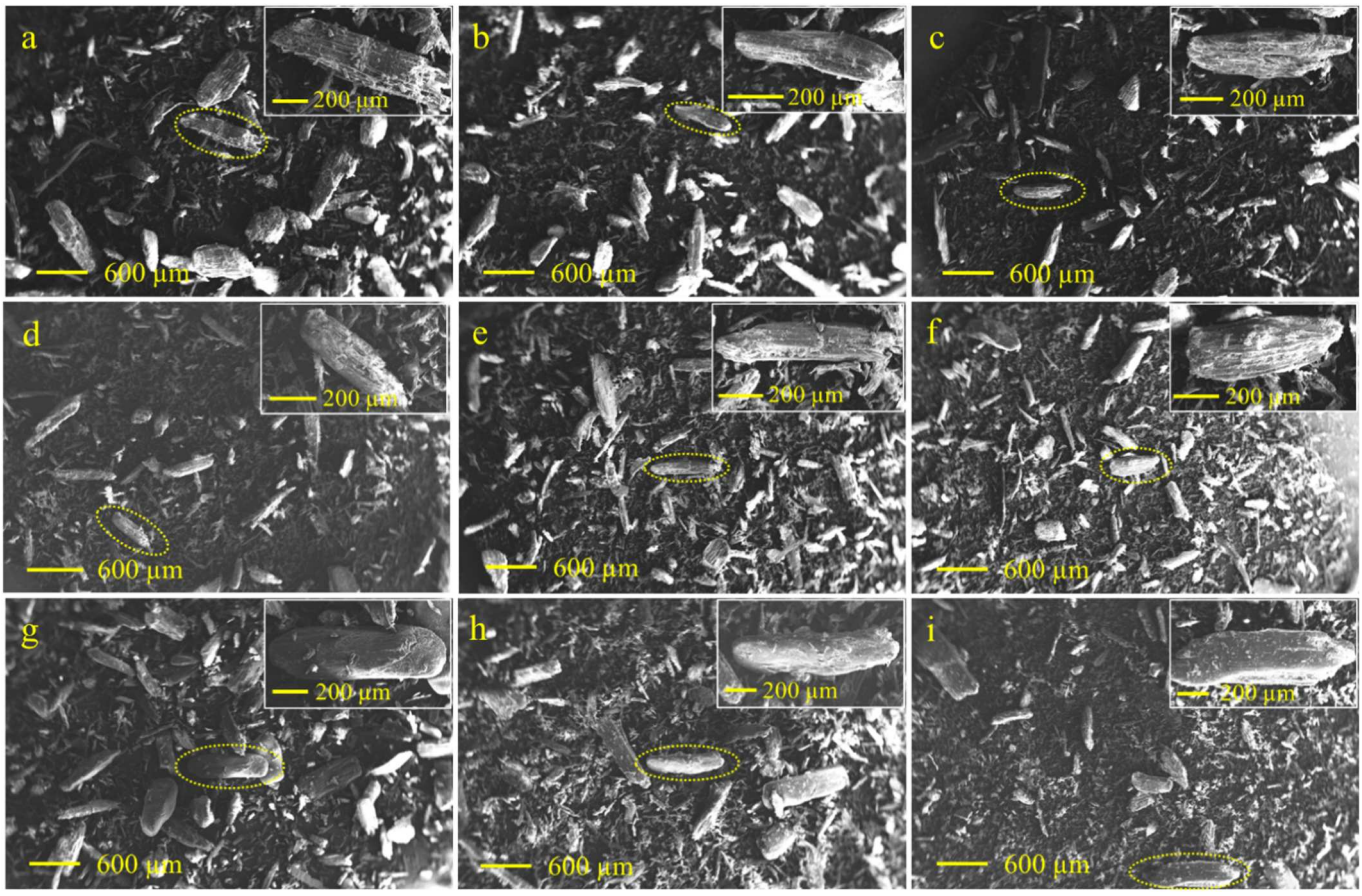

Figure 1. SEM images of the WFs: (a) L15-0M, (b) L15-6M, (c) L15-12M, (d) L30-0M, (e) L30-6M, (f) L30-12M, (g) L39-0M, (h) L39-6M, and (i) L39-12M.

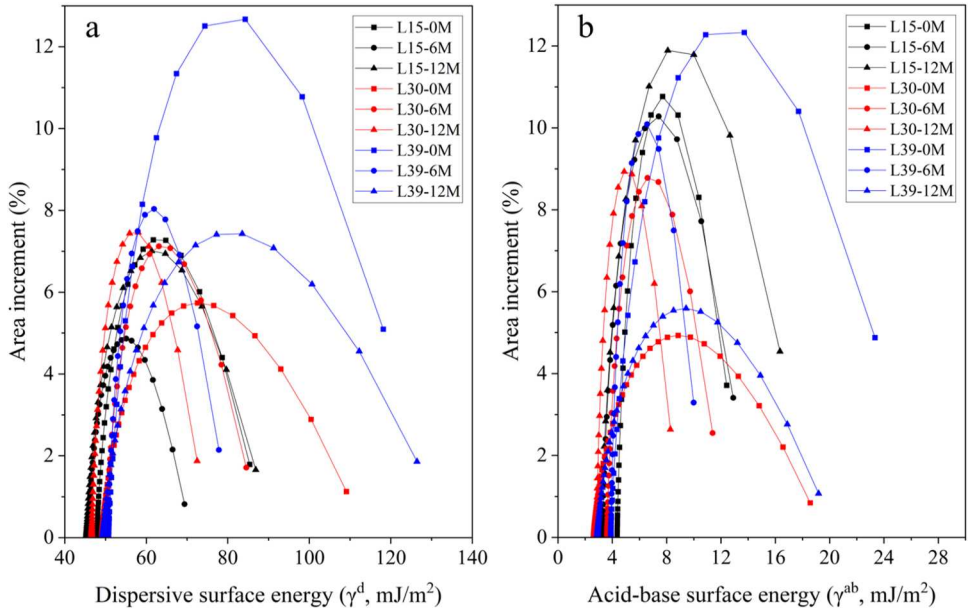

Figure 2. Dispersive and acid-base surface energy distributions of the WFs.

exposure, the WFs from the 39-year-old tree showed significantly higher surface energies than those from the 30-year-old tree, followed by the 15-year-old tree. The increase in the dispersive and acid–base components with tree maturity is mainly attributed to changes in chemical composition. As the tree grows, greater amounts of extractives and cellulose develop, which contribute to the enhancement of the dispersive and acid–base components, respectively.

After environmental exposure, the dispersive component of the WFs from the 15- and 39-year-old trees initially decreased after 6 months of exposure but subsequently increased after 12 months. In contrast, the WFs from the 30-year-old tree exhibited a continuous decline in the dispersive component with increasing exposure duration from 0 to 12 months. This differing trend in the dispersive component is likely associated with the relatively high lignin and extractive contents in the younger (15-year-old) and older (39-year-old) trees, respectively. In the early stage of exposure, the leaching of hydrophobic extractives resulted in a decrease in the dispersive component, whereas during prolonged exposure, the accumulation of condensed oxidized lignin or extractive fragments may contribute to its subsequent increase. A similar trend was observed in the acid–base component, where the loss of hemicellulose likely caused the initial decrease, and the formation of hydrophilic fragments from the oxidation of lignin and extractives led to a later increase in the WFs from the 15- and 39-year-old trees.

Both dispersive and acid–base surface energies can critically influence the interfacial behavior and performance of PP/WF composites. Higher dispersive energy, mainly from lignin and extractives, may slightly improve fiber dispersion in hydrophobic matrices through nonpolar interactions when compatibilizers are absent. However, the inherently hydrophilic nature of WFs can limit their compatibility with nonpolar polymers, leading to fiber agglomeration and weak fiber-matrix interactions. To achieve better compatibility, the use of reactive compatibilizers is essential. Higher acid–base components of the surface energy, mainly from cellulose and hemicellulose, can provide more reactive sites for interaction with compatibilizers, thereby enhancing fiber-matrix adhesion. The final composite properties also depend on factors such as fiber strength, aspect ratio, processing conditions, and matrix characteristics.

3.2. Mechanical properties

3.2.1. Impact strength

The three-way ANOVA results (Table S1) illustrate the relative influence of each factor on impact strength, as quantified by the F-value for the main effects, which indicates their contribution to the variability in impact strength. Among the factors, tree age (F = 870) was the most dominant, followed by loading level (F = 190), while exposure duration (F = 2.50) had the least significant effect. However, the presence of a significant three-way interaction (tree age × exposure duration × loading level, $p < 0.0001$) indicates that the impact of each factor depends on the levels of the other two. This suggests that analyzing these factors independently, without considering their interactions, may lead to incomplete interpretations.

To fully understand these relationships, Tukey's HSD post-hoc tests should ideally be conducted by holding two factors constant while comparing the levels of the third factor. As this study aimed to capture overall trends rather than isolate interaction effects, Tukey's HSD comparisons were performed as follows: (1) For tree age and loading level, only within the 0-month group, since unexposed trees were unaffected by exposure duration; (2) for exposure duration, comparisons were made separately for each tree age group. The impact strength measurement results are shown in Figure 3, while the detailed mean comparison results are provided in Tables S8 to S11.

The impact strength of neat PP was 1.49 kJ/m^2. After reinforcement with WFs, all composites exhibited significant increases in impact strength, with the highest improvement observed in the L30-12M-50% composite, which showed a 132% increase. This enhancement is attributed to WFs serving as stable reinforcements with the assistance of MAPP compatibilizer. As shown in Figure 4 (the original SEM images are provided in Figures S22 to S24), the fractured composite surface was much rougher than that of neat PP, with visible fractured WFs, indicating their role in sustaining impact stress and enhancing the composites' toughness.

The composites reinforced with WFs from different trees exhibited a clear trend in impact strength: L30 > L15 > L39, regardless of the loading level. Compared to the 15-year-old tree, WFs from the 30-year-old tree, with a higher maturity level, developed lower microfibril angles, enhancing their ability to dissipate impact energy in the composites (Via *et al.* 2009). However, WFs from the 39-year-old tree contained a higher concentration of extractives, such as resins, tannins, and waxes, which created localized weak spots in the composites. These weak regions acted as stress concentrators, facilitating the initiation and propagation of cracks, ultimately leading to premature failure.

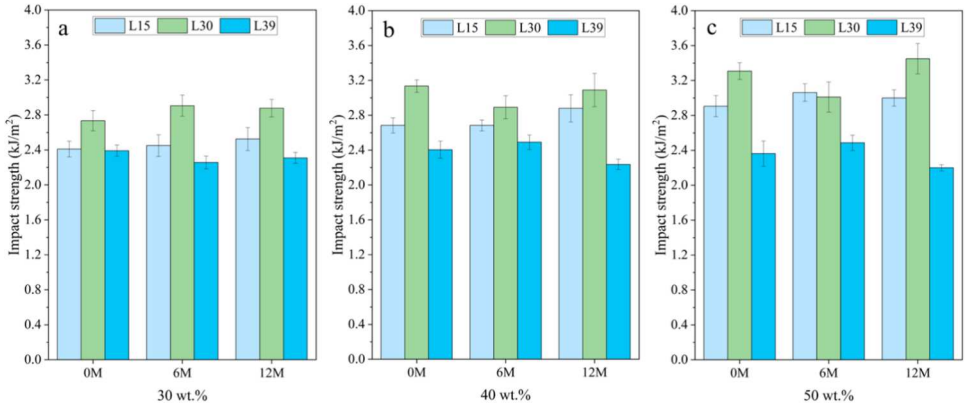

Figure 3. Impact strength of the PP/WF composites.

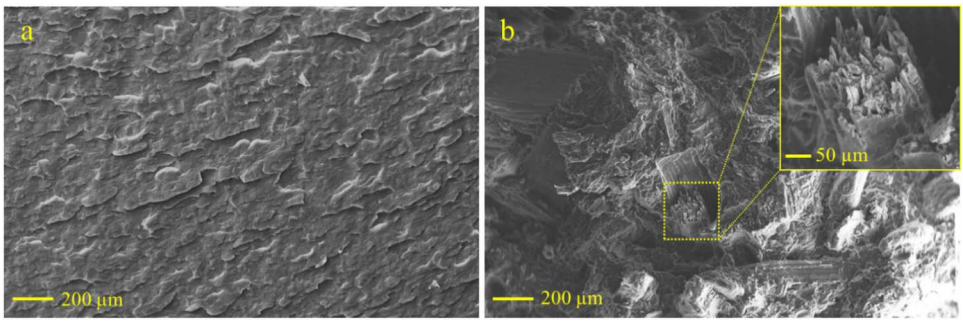

Figure 4. SEM images of the fractured surfaces of (a) neat PP and (b) the L30-12M-50% composite.

For composites reinforced with WFs from 15- and 30-year-old trees, impact strength significantly increased with higher loading levels. However, composites reinforced with WFs from the 39-year-old tree exhibited comparable impact strength across all three loading levels. This could also be attributed to the increased extractives. Moreover, as observed earlier in Figure 2(b), the higher acid–base surface energy of the 39-year-old tree's fibers may have intensified fiber-fiber interactions, promoting fiber agglomeration and causing early fiber saturation, consequently limiting further reinforcement.

For the 15-year-old tree, impact strength showed no significant differences across exposure durations at 30 and 50 wt.% loading levels. However, at 40 wt.% loading, composites reinforced with WFs from 12-month environment-exposed timber exhibited higher impact strength than those from 0- and 6-month exposure. For the 30-year-old tree, exposure duration had no effect at 30% loading, while at 40 and 50 wt.% loadings, composites reinforced with WFs from 0- and 12-month exposure displayed similar impact strength, both of which were higher than the 6-month exposure. In contrast, the 39-year-old tree showed a different pattern. At 30 wt.% loading, composites reinforced with WFs from 0- and 12-month exposure had similar impact strength, while the 6-month exposure resulted in slightly lower values. At the 40 wt.% loading, 0- and 6-month exposures yielded comparable impact strengths, whereas 12-month environmental exposure significantly reduced it. At 50 wt.% loading, impact strength followed the trend: 6 months > 0 months > 12 months.

The effect of exposure duration varied with tree age and loading level; however, a noticeable trend was observed. 12-month exposure generally enhanced impact strength in younger trees (15- and 30-year-old) but reduced it in older trees (39-year-old). A possible explanation is that in younger trees, extended exposure led to the leaching of a small amount of extractives, while the oxidation introduced additional hydroxyl (-OH), carboxyl (-COOH), and carbonyl (C = O) groups on the fiber surface, collectively enhancing fiber wettability and improving fiber-matrix interactions. However, in older trees, the loss of a large amount of extractives made the fibers more susceptible to microbial activity, which disrupted the integrity of the wood cell structure through molecular fragmentation and cleavage of hemicellulose and lignin, increasing the number of microcracks and stress concentration points, ultimately weakening the composite's performance.

Overall, the exposure duration had a less consistent and less pronounced effect on impact strength, suggesting that the timeframe for salvaging downed timbers can remain flexible without significant concern that prolonged exposure in the forest land will severely degrade fiber performance for reinforcing PP composites.

3.2.2. Tensile properties

Similarly, three-way ANOVA results (Table S2 to S4) show the main effects of tree age, exposure time, and loading level on tensile strength, MOE, and strain. For tensile strength, tree age exhibited the most dominant effect (F = 2341), significantly outweighing the effects of exposure time (F = 303) and loading level (F = 255). In contrast, for MOE, loading level was the primary influencing factor (F = 1257), while tree age (F = 20.7) and exposure time (F = 63.5) had relatively minor effects. For tensile strain, the effects followed the order: tree age (F = 812) > fiber loading level (F = 667) > exposure time (F = 78.6). The tensile properties are shown in Figure 5, their detailed mean comparisons were conducted using the same method as for impact strength, and the results are presented in Table S12-23.

Compared to the tensile strength of PP (30.9 MPa), most composites exhibited notable enhancements, except for those reinforced with WFs from the unexposed and 12-month-exposed 39-year-old tree, likely due to the high extractive content and fiber deterioration, respectively, as discussed in the impact results. The L30-12M-50% composite exhibited the highest enhancement, with a 50.2% increase in tensile strength. At 30 wt.% loading, the composite reinforced with 15-year-old tree WFs exhibited higher tensile strength than that reinforced with 30-year-old tree WFs. At the 40 wt.% loading, both composites showed similar tensile strength, while at the 50 wt.% loading, the composite reinforced with 30-year-old tree WFs demonstrated greater tensile strength than the one reinforced with 15-year-old tree WFs. This inconsistency stems from the fact that, during tensile testing, both WFs had high intrinsic strength, and instead of fiber fracture, most failures occurred at the fiber-matrix interface. Given the minor differences in surface properties between the WFs and the same MAPP compatibilizer content, variations in interfacial adhesion were minimal. Therefore, the inconsistent trend across different tree ages is likely due to the random distribution of natural fiber defects or extractives, which acted as fracture initiation points within the composites. This factor

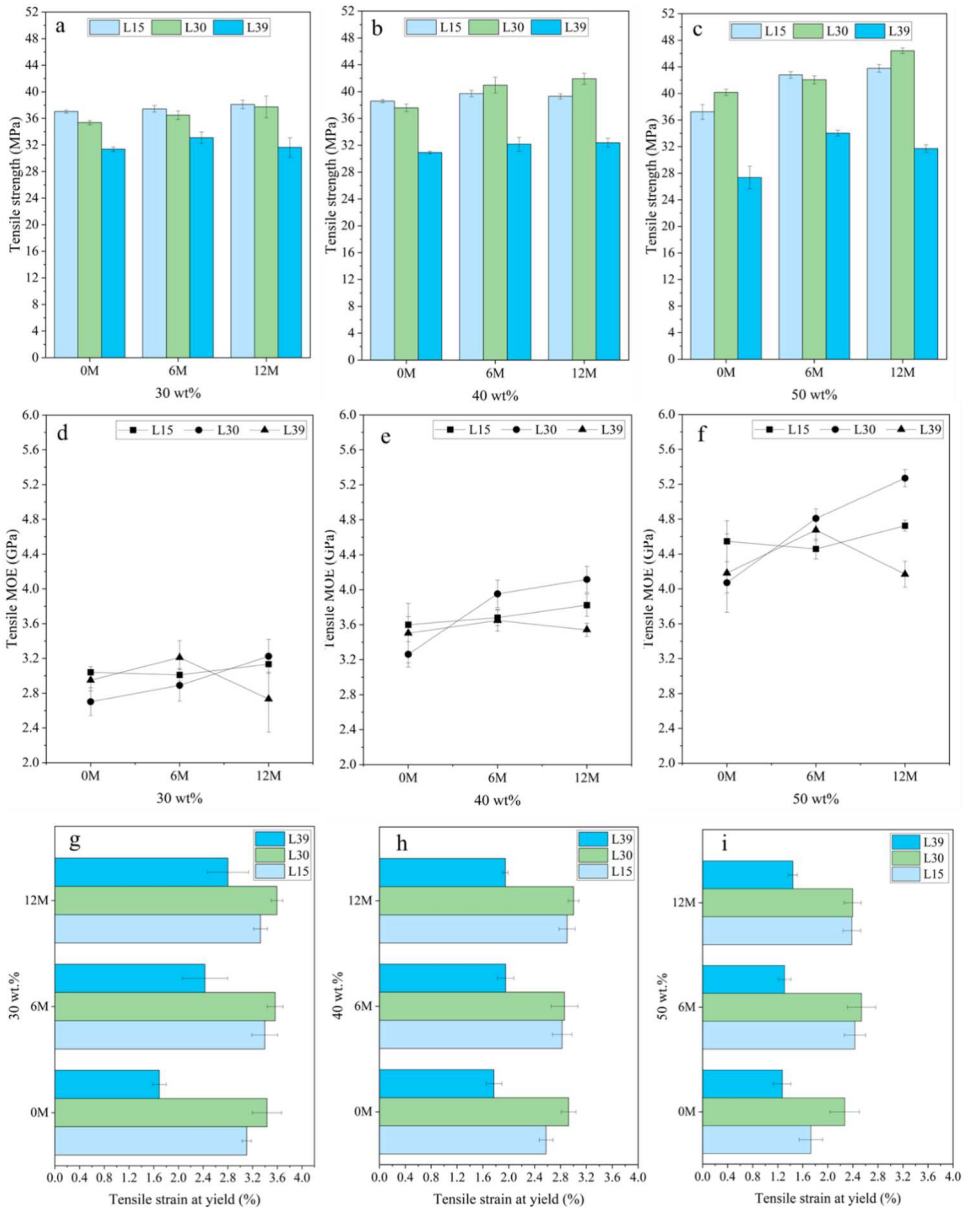

Figure 5. Tensile strength, MOE, and strain at yield of the PP/WF composites.

could also explain the variability observed in the effect of loading level. Whereas all composites reinforced with 39-year-old tree WFs, regardless of loading level, exhibited significantly lower tensile strength than those reinforced with 15- and 30-year-old tree WFs, which can be attributed to the former's higher likelihood to form clustered agglomerations. For the effect of exposure duration, a trend similar to that observed in the impact strength results, but more pronounced, was found. Composites reinforced with WFs from extended-exposure timbers exhibited higher tensile strength for the 15- and 30-year-old trees but lower tensile strength for the 39-year-old tree.

Compared to PP's MOE (1.60 GPa), all composites exhibited distinct improvements, with the highest enhancement of 229% observed in the L30-12M-50% composite. The composites' MOE was not significantly influenced by tree age, whereas the loading level had a pronounced effect, with higher loadings leading to increased stiffness due to the inherently high rigidity of all WFs. Notably, the WFs from the timber subjected to 12-month exposure consistently enhanced the stiffness of composites in younger trees (15- and 30-year-old).

The flexibility of the composites was evaluated based on their tensile strain at yield. Neat PP exhibited a tensile strain at yield of 8.22%, while the incorporation of WFs reduced the composites' flexibility, as indicated by the decreased strain at yield. The WFs from the 30-year-old tree resulted in the least reduction, likely due to their proper fiber maturity. Additionally, higher loading levels led to a greater decrease in tensile strain.

3.2.3. Flexural properties

The three-way ANOVA results (Tables S5 to S7) revealed trends similar to those observed in the tensile properties, with tree age being the dominant factor affecting flexural strength, while

loading level had the most significant influence on flexural MOE and strain.

According to the measured properties (Figure 6) and the detailed mean comparison results (Tables S24 to S35), similar general trends were found: (1) the WF addition contributed to increased flexural strength, following the pattern L30 > L15 > L39; (2) higher loading levels generally enhanced flexural strength, except in composites reinforced with 39-year-old tree WFs, where saturation occurred at lower loading levels; (3) extended exposure duration improved WFs' reinforcing capacity, increasing both strength and MOE for younger trees (15- and 30-year-old); (4) tree age had a minor influence on MOE; (5) higher loading levels consistently led to higher MOE; and (6) the WF addition reduced flexibility of the composite, with composites reinforced with 30-year-old tree WFs experiencing the least decline.

3.3. Rheological properties

3.3.1. Complex viscosity

Rheological measurements were conducted to further investigate fiber-matrix interactions and gain insight into the flow behavior and processability of the composites. The plots of complex viscosity versus angular frequency are shown in Figure 7. Additionally, alternative plots of the same data with enhanced visualization for comparing different exposure durations are provided in Figure S1. All composites, except for the L39-12M-30%, exhibited higher complex viscosity than neat PP, indicating that the addition of WFs reduced the flowability of the polymer matrix due to enhanced stiffness and fiber-polymer interactions. The exception of decreasing viscosity observed for the L39-12M-30% is due to the severe deterioration of the fibers from the older tree, likely caused

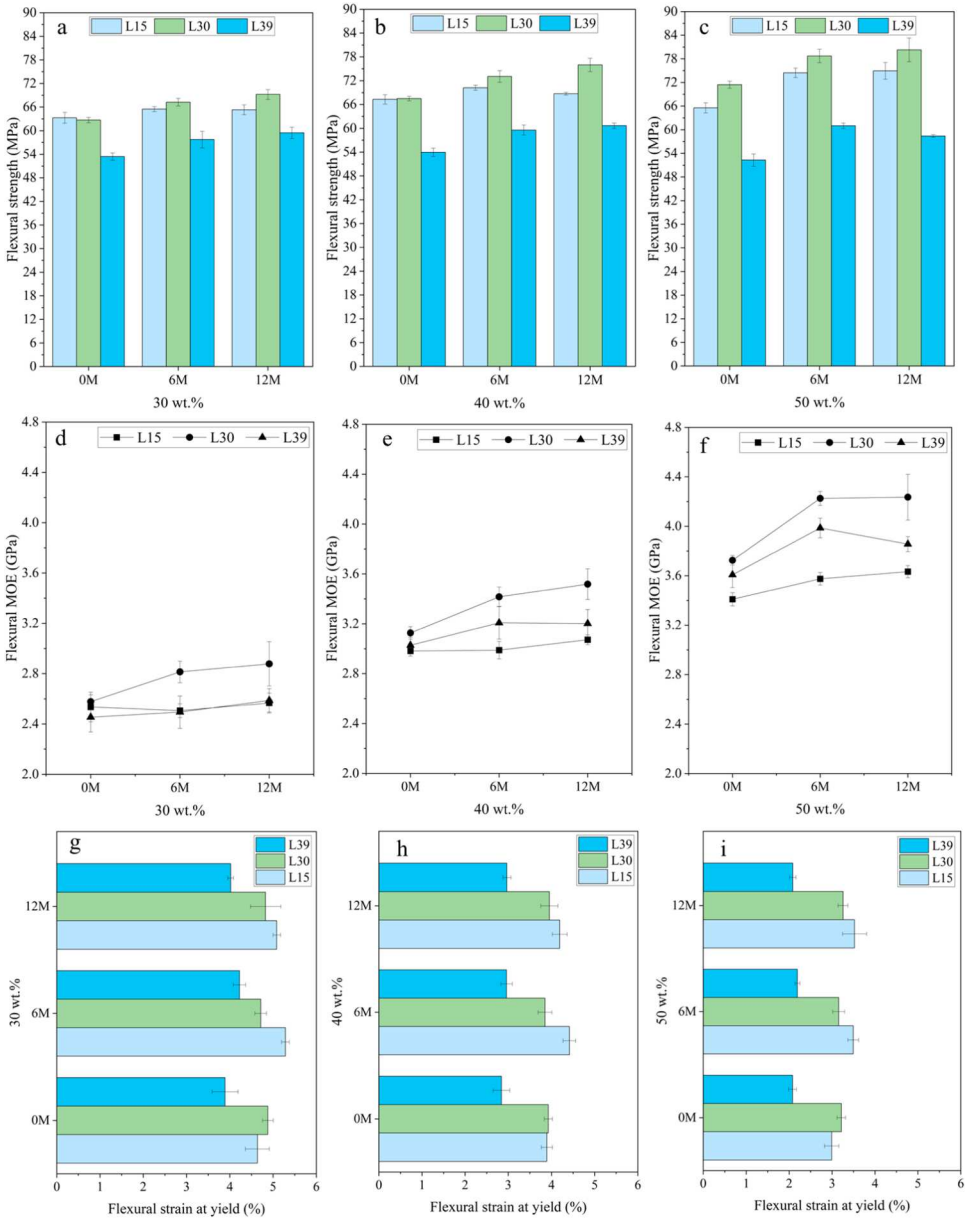

Figure 6. Flexural strength, MOE, and strain at yield of the PP/WF composites.

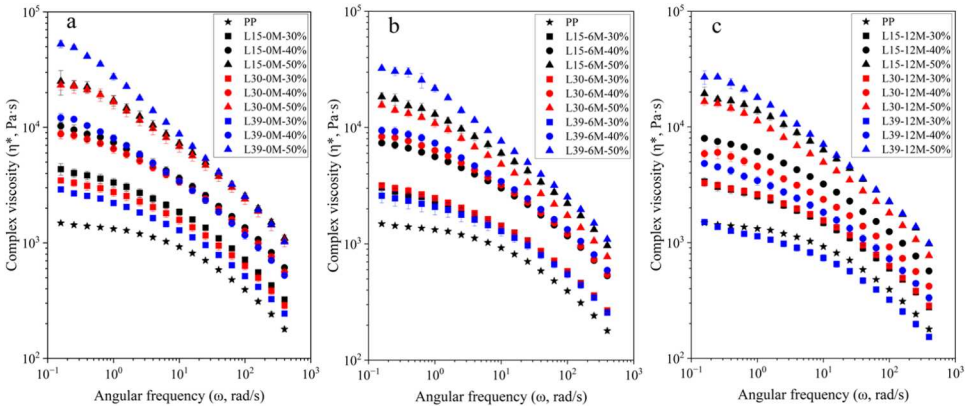

Figure 7. Complex viscosity of the PP/WF composites.

by oxidative or microbial degradation of the WFs after 12 months of environmental exposure, including the loss of hemicellulose and destruction of structural integrity. Higher loading levels consistently resulted in higher complex viscosity, regardless of tree age and exposure duration. This increased viscosity indicates reduced processability, potentially resulting in higher energy consumption, poor fiber dispersion, and an increased risk of equipment wear during processing. Therefore, a careful balance between composite performance and processability must be considered in real-world manufacturing processes.

Before environmental exposure, at 50 and 40 wt.% loading levels, the composite with WFs from the 39-year-old tree showed higher viscosity values than those with WFs from the 30- and 15-year-old trees. However, at the 30 wt.% loading level, the composite with WFs from the 39-year-old tree exhibited a lower viscosity than the composites with WFs from the 30- and 15-year-old trees. This indicates that the impact of tree age on composite viscosity is not independent of the loading level. After environmental exposure, the viscosity of the composite containing 50 wt.% WFs from the 39-year-old tree decreased markedly, from 5.26 $x10^4$ Pa·s at 0 month to 3.23 $x10^4$ Pa·s after 6 months and further to 2.69 $x10^4$ Pa·s after 12 months at the initial low shear rate (0.16 rad s^{-1}). The only change is that the fiber quality and environmental exposure changed the quality of the WFs, which resulted in the lower viscosity of the composite. This also applies to composites with loading levels of 40 and 30 wt.%, where viscosity decreased from 1.21 $x10^4$ to 0.94 $x10^4$ and 0.48 $x10^4$ Pa·s, and from 2.90 $x10^3$ to 2.59 $x10^3$ and 1.51 $x10^3$ Pa·s after 6 and 12 months of exposure, respectively. These changes also indicate that the viscosity data at low shear rate can be used to probe the fiber quality or the interaction between fibers and polymers. Similarly, for the composites with WFs from the 30- and 15-year-old trees, environmental exposure led to a decrease in viscosity after 6 months; however, with further exposure to 12 months, no significant decline in viscosity was observed for most composites, regardless of loading level. This indicates that the fiber quality deteriorates more rapidly in the older tree (39 years old) than in the younger trees (30 and 15 years old) under environmental exposure.

Notably, after six months of environmental exposure to the WFs, the viscosity values of composites L39-6M-40% and L30-6M-40% are higher than those of L15-6M-40%. However, after exposing WFs to 12 months of the environment, the viscosity values of the composites of L39-12M-40% and L30-12M-40% are lower than those of L15-12M-40%. This observation indicated that the deterioration of WFs for trees of different ages is significantly different. Further analysis, however, showed that the viscosity of composites at the 50 wt.% loading level has similar viscosity changes due to the addition of WFs, i.e. the viscosity values of composites L39-12M-50% and L15-12M-50% are higher than that of L30-12M-50%, as observed with the effects of the WFs exposed to the environment for 6 months at 50 wt.%. This observation indicates that the loading level of the WFs at the 50 wt.% dominate the impact on the viscosity of the composites. At the WF loading level of 40 wt.%, other factors, such as the interaction between polymer and WFs or the quality (stiffness) of the WFs, may dominate the effect on the viscosity of the composites.

Overall, variations in complex viscosity were observed in relation to both tree age and exposure duration; however, their impacts were significantly less pronounced compared to the effect of loading level. Therefore, from a composite manufacturing and processing standpoint, the influences of tree age and exposure duration may require less consideration when utilizing WFs from the downed timber for reinforcing PP composites.

3.3.2. Storage and loss moduli

Figure 8, along with Figure S2, presents the storage and loss moduli as functions of angular frequency. The loading level was the most dominant factor influencing the composites' elastic behavior; higher loading levels resulted in higher storage and loss moduli. Compared with neat PP, all composites exhibited distinctly higher storage moduli in the low-frequency region ($\omega < 1$ rad s^{-1}), indicating that the incorporation of WFs enhanced stress transfer and load-bearing capability, as further supported by the increased tensile and flexural strength and MOE relative to neat PP. The addition of WFs also enhanced the composites' energy dissipation ability, as evidenced by the increased loss modulus, except for the composites containing WFs from the 39-year-old tree exposed for 12 months at the 30 wt.% loading level. This enhancement was consistent with the improvement in impact resistance. The increases in storage and loss moduli

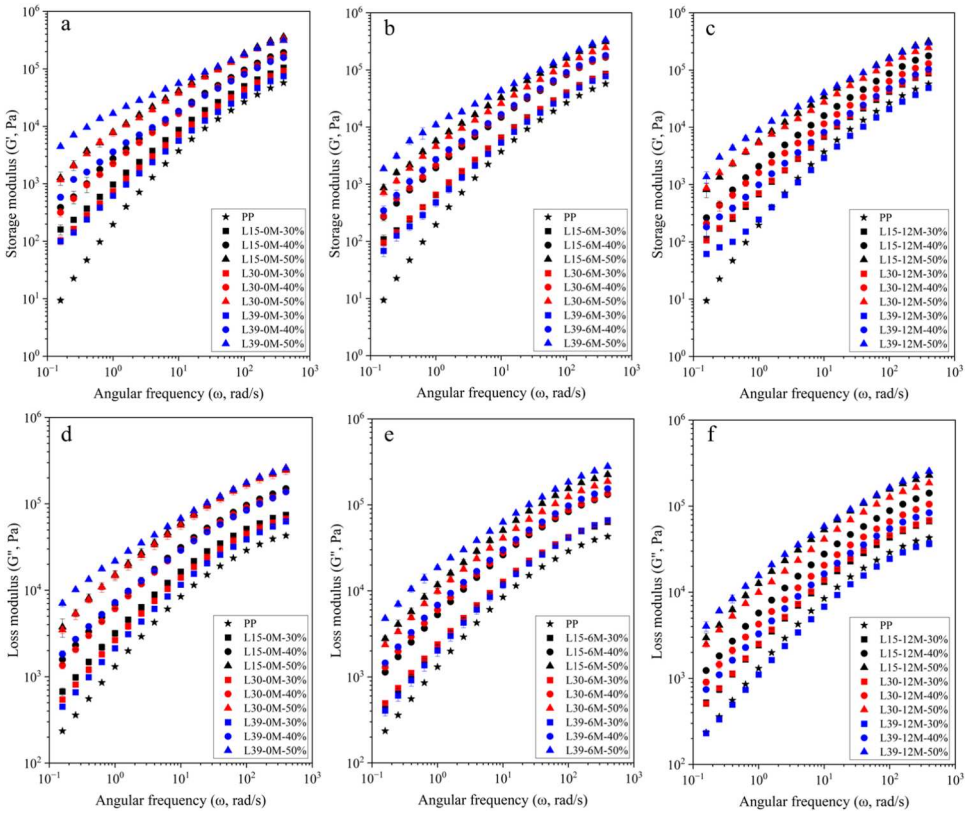

Figure 8. Storage and loss moduli of the PP/WF composites.

were attributed to the presence of WFs and the MAPP compatibilizer, which strengthened the fiber-fiber and fiber-polymer interactions, facilitating greater energy storage and dissipation through strong interfacial bonding via MAPP and internal friction among rigid fibers. For the composite with WFs from the 39-year-old tree exposed for 12 months at the 30 wt.% loading level, the observed decrease in loss modulus was attributed to fiber degradation, such as the loss of hemicellulose or partial lignin. This degradation weakened fiber-polymer interactions, allowing fiber slippage within the polymer matrix and thereby reducing frictional resistance. Additionally, the loss of hemicellulose or lignin increased the ratio of crystalline to amorphous regions, thereby enhancing the crystallinity of the WFs. As a result, the fibers became less flexible, which contributed to the decreased loss modulus in the composite's rubbery state (Hosseinaei *et al.* 2012).

Similar trends to those observed for complex viscosity were found in the storage and loss moduli with respect to tree age and exposure duration. Before environmental exposure, at 50 and 40 wt.% loading levels, the composites with WFs from the 39-year-old tree exhibited higher storage and loss moduli compared with those from the 30- and 15-year-old trees. However, at the 30 wt.% loading level, the composite with WFs from the 39-year-old tree showed lower storage and loss moduli than those with WFs from the younger trees. This behavior is likely due to an interplay between the effects of loading level and tree age, with tree age determining the intrinsic fiber quality. At the 30 wt.% loading level, fiber quality predominantly governed the composite's viscosity. Moreover, extended environmental exposure reduced the storage and loss moduli of the composites by weakening fiber-polymer interactions, resulting from fiber degradation, with the composites containing WFs from the 39-year-old tree exhibiting a more pronounced reduction.

3.3.3. Phase angles

The phase angle results (Figures 9 and S3) are provided to analyze the damping behavior of the composites, offering insights into the optimization of processing and composite performance. The variations in phase angles in response to loading level, tree age, and exposure duration largely followed the same trends observed in complex viscosity, storage modulus, and loss modulus for the same reasons.

More importantly, all composites exhibited viscoelastic liquid behavior at angular frequencies below 100 rad/s, which benefits low-to-moderate shear processing methods such as melt compounding and compression molding by ensuring sufficient flowability for efficient fiber dispersion, thereby improving process efficiency and promoting a uniform composite structure. At angular frequencies above 100 rad/s, all composites transition to a more viscoelastic solid behavior, preventing excessive deformation and enhancing shape retention. This minimizes dimensional inconsistencies in high-shear processing methods such as extrusion, injection molding, and large-scale extrusion-based additive manufacturing, making the composites well-suited for scalable construction materials and other engineering applications. Across the tested frequency range, the composites exhibited viscoelastic trends broadly similar to neat PP, suggesting no unusual melt response under these small-amplitude oscillatory conditions.

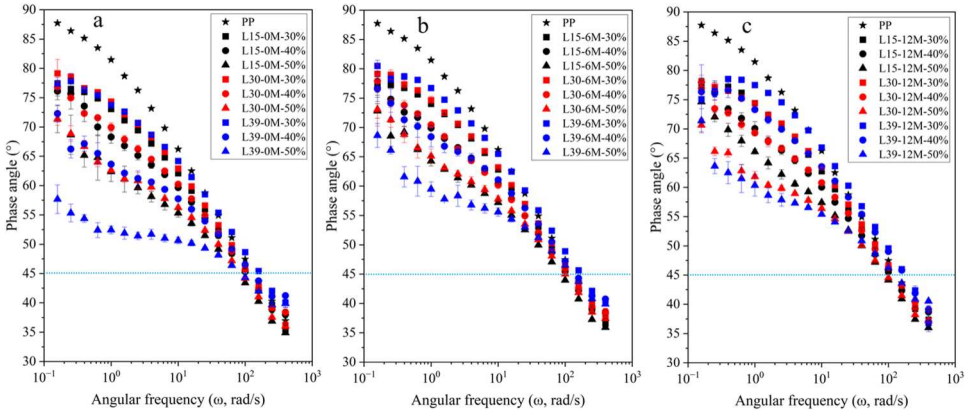

Figure 9. Phase angles of the PP/WF composites.

4. Conclusions

The size, morphology, and surface properties of the WFs obtained from downed timber of various tree ages and environmental exposure durations were investigated, and subsequently, the WFs at different loading levels were examined as reinforcing agents for PP.

Tree age had a limited influence, while extended environmental exposure resulted in a relatively higher proportion of finer particles. The higher extractive content in the 39-year-old tree made its fiber surface smoother and increased its dispersive and acid–base energies. However, after environmental exposure, these energies decreased due to extractive leaching, lignin oxidation, and microbial activity.

All WFs effectively reinforced PP, with the optimal mechanical performance observed in the L30-12M-50% composite. The age of the tree was found to critically affect the mechanical properties of the composites, with performance following the order L30 > L15 > L39. The high maturity of L30 contributed to enhanced performance, while the high extractive content of L39 made its fibers prone to agglomeration. Environmental exposure had a less pronounced effect on the mechanical properties of composites reinforced with fibers from 15- and 30-year-old trees but had a distinct impact on those reinforced with fibers from 39-year-old trees. A higher loading level significantly increased composite stiffness, with the 50 wt.% loading level having the most substantial effect on the rheological properties of composites reinforced with 39-year-old tree fibers. The rheological behavior of these composites consistently supported the trends observed in mechanical performance while further revealing fiber-matrix interactions, with their processability also evaluated based on viscoelastic responses.

Acknowledgements

We acknowledge ExxonMobil Chemical Company for providing PP pellets. Ke Zhan: Methodology, investigation, data curation, formal analysis, visualization, writing - original draft, writing - review & editing. Courtney Higgins: Data curation, formal analysis. Mi Li: Data curation, formal analysis, resources. Mathew Smidt: Resources. Thomas Elder: Writing - review & editing, resources. Wei Gao: Writing - review & editing. Yucheng Peng: Conceptualization, methodology, investigation, writing - review & editing, resources, supervision, funding acquisition.

Author contributions

CRediT: **Ke Zhan:** Data curation, Formal analysis, Investigation, Methodology, Visualization, Writing – original draft, Writing – review & editing; **Courtney Higgins:** Data curation, Formal analysis; **Mi Li:** Data curation, Formal analysis; **Mathew Smidt:** Resources; **Thomas Elder:** Resources, Writing – review & editing; **Wei Gao:** Writing – review & editing; **Yucheng Peng:** Conceptualization, Funding acquisition, Investigation, Methodology, Resources, Supervision, Writing – review & editing.

Disclosure statement

No potential conflict of interest was reported by the author(s).

Funding

This study was financially supported by the USDA Forest Service Southern Research Station (Downed Timber Research Program G00013505) and the USDA National Institute of Food and Agriculture (McIntire Stennis project ALAZ00079).

Data availability statement

Data will be made available on reasonable request.

References

Aghalari, A., *et al.*, 2021. A bilevel model formulation for solving a post-hurricane damaged timber management problem. *Computers & Industrial Engineering*, 162, 107726.

Aladwan, B.S., 2021. *Optimizing a biomass supply system: consideration of pellet quality and transportation under extreme events*. Mississippi, United States: Mississippi State University.

Andrzejewski, J., *et al.*, 2024. Manufacturing and characterization of sustainable and recyclable wood-polypropylene biocomposites: multiprocessing-properties-structure relationships. *Industrial Crops and Products*, 207, 117710.

Ayana, K.D., Ha, C.-S., and Ali, A.Y., 2024. Comprehensive overview of wood polymer composite: formulation and technology, properties, interphase modification, and characterization. *Sustainable Materials and Technologies*, 40, e00983.

Bao, F.C., *et al.*, 2001. Differences in wood properties between juvenile wood and mature wood in 10 species grown in China. *Wood Science and Technology*, 35, 363–375.

Basiji, F., *et al.*, 2025a. Impact of fiber morphology and content on the thermal stability, and mechanical performance of maple wood fiber-polypropylene composites. *Journal of Applied Polymer Science*, 142, e57211.

Basiji, F., *et al.*, 2025b. Influence of fiber concentration and length on the dielectric, mechanical, and thermal properties of maple wood fiber-reinforced polypropylene. *Journal of Thermoplastic Composite Materials*, 38, 3739–3780.

Ben Hamou, K., *et al.*, 2023. Synergistic association of wood /hemp fibers reinforcements on mechanical, physical and thermal properties of polypropylene-based hybrid composites. *Industrial Crops and Products*, 192, 116052.

Bledzki, A.K., and Faruk, O., 2003. Wood fibre reinforced polypropylene composites: effect of fibre geometry and coupling agent on physico-mechanical properties. *Applied Composite Materials*, 10, 365–379.

Broda, M., and Popescu, C.-M., 2019. Natural decay of archaeological oak wood versus artificial degradation processes — an FT-IR spectroscopy and X-ray diffraction study. *Spectrochimica Acta Part A: Molecular and Biomolecular Spectroscopy*, 209, 280–287.

Callaghan, J., 2025. Disastrous effects of Hurricane Helene in the Southern Appalachian Mountains including a review of mechanisms producing extreme rainfall. *Hydrology*, 12, 201.

Clark, A., Daniels, R.F., and Jordan, L., 2006. Juvenile/mature wood transition in loblolly pine as defined by annual ring specific gravity, proportion of latewood, and microfibril angle. *Wood and Fiber Science*, 38 (2), 292–299.

Corkran, R., Trepanier, J., and Brown, V., 2024. Spatiotemporal climatology of Georgia tropical cyclones and associated rainfall. *Journal of Marine Science and Engineering*, 12 (10), 1693.

Daniel, G., 2014. Fungal and bacterial biodegradation: white rots, brown rots, soft rots, and bacteria. In: *Deterioration and protection of sustainable BiomaterialsAmerican chemical society* T.P. Schultz, B. Goodell and D.D. Nicholas, eds. Uppsala: American Chemical Society, pp. 23–58.

Erchiqui, F., *et al.*, 2008. Investigation of relaxation properties and potentiality of the thermoformability of HDPE charged by wood flours. *Journal of Reinforced Plastics and Composites*, 28, 1153–1168.

Erchiqui, F., *et al.*, 2009. Engineering investigations on the potentiality of the thermoformability of HDPE charged by wood flours in the thermoforming part. *Polymer Engineering & Science*, 49, 1594–1602.

Ferdinánd, M., *et al.*, 2023. Impact modification of wood flour reinforced PP composites: problems, analysis, solution. *Composites Part A: Applied Science and Manufacturing*, 167, 107445.

Gao, C., Cui, X., and Matsumura, J., 2024. Multidimensional exploration of wood extractives: a review of compositional analysis, decay resistance, light stability, and staining applications. *Forests*, 15 (10), 1782.

Gardner, D.J., Han, Y., and Wang, L., 2015. Wood–plastic composite technology. *Current Forestry Reports*, 1, 139–150.

Goodell, B., Winandy, J.E., and Morrell, J.J., 2020. Fungal degradation of wood: emerging data, new insights and changing perceptions. *Coatings*, 10 (12), 1210.

Gunwant, D., 2024. Moisture resistance treatments of natural fiber-reinforced composites: a review. *Composite Interfaces*, 31, 979–1047.

Guo, J., Prestemon, J., and Johnston, C., 2023. Forest market outlook in the Southern United States. *Forest Policy and Economics*, 157, 103091.

He, L., *et al.*, 2016. Regional woody biomass supply and economic impacts from harvesting in the southern U.S. *Energy Economics*, 60, 151–161.

Hernandez-Diaz, J.A., *et al.*, 2024. Wavelet analysis and forecasting using open-access lumber market indices for assessing the impact of hurricanes on Southern US stumpage prices. *Forest Products Journal*, 74, 10–27.

Hillis, W.E., 1971. Distribution, properties and formation of some wood extractives. *Wood Science and Technology*, 5, 272–289.

Hosseinaei, O., *et al.*, 2012. Effects of hemicellulose extraction on properties of wood flour and wood–plastic composites. *Composites Part A: Applied Science and Manufacturing*, 43, 686–694.

Hristov, V.N., *et al.*, 2004. Deformation mechanisms and mechanical properties of modified polypropylene/wood fiber composites. *Polymer Composites*, 25, 521–526.

Janusz, G., *et al.*, 2017. Lignin degradation: microorganisms, enzymes involved, genomes analysis and evolution. *FEMS Microbiology Reviews*, 41, 941–962.

Karasinski, M.A., *et al.*, 2023. *Integrating Nasa's Gedi and Landsat 8 Oli data for regional aboveground biomass mapping in forested areas impacted by Hurricane Ian in Florida*. IEEE.

Khodayari, A., *et al.*, 2021. Cellulose-hemicellulose interactions - a nanoscale view. *Carbohydrate Polymers*, 270, 118364.

Kirker, G.T., *et al.*, 2013. The role of extractives in naturally durable wood species. *International Biodeterioration & Biodegradation*, 82, 53–58.

Kirker, G.T., *et al.*, 2024. Critical review on the use of extractives of naturally durable woods as natural wood protectants. *Insects*, 15 (1), 69.

Liu, W., *et al.*, 2024. A novel approach to manufacturing high-performance reclaimed carbon fiber composites via convergent flow-induced discontinuous fiber aligned placement (CFi-DFAP). *Composites Part B: Engineering*, 271, 111178.

Lu, C., *et al.*, 2021. Influence of juvenile and mature wood on anatomical and chemical properties of early and late wood from Chinese fir plantation. *Journal of Wood Science*, 67, 72.

Martín, J.A., and López, R., 2023. Biological deterioration and natural durability of wood in Europe. *Forests*, 14(2), 283.

Martínez, Á.T., *et al.*, 2005. Biodegradation of lignocellulosics: microbial, chemical, and enzymatic aspects of the fungal attack of lignin. *International Microbiology*, 8, 195–204.

Miranda, I., and Pereira, H., 2002. The variation of chemical composition and pulping yield with age and growth factors in young Eucalyptus globulus. *Wood and Fiber Science*, 34 (1), 140–145.

Mohammadi, N., *et al.*, 2011. Studying the effect of the age of a tree on chemical composition and degree of polymerization cellulose. *Indian Journal of Science and Technology*, 4, 1679–1680.

Moore, T.R., *et al.*, 2015. Quantifying changes in extreme weather events in response to warmer global temperature. *Atmosphere-Ocean*, 53, 412–425.

Park, B.-D., and Balatinecz, J.J., 1997. Mechanical properties of wood-fiber/toughened isotactic polypropylene composites. *Polymer Composites*, 18, 79–89.

Pérez, E., *et al.*, 2012. Tensile and fracture behaviour of PP/wood flour composites. *Composites Part B: Engineering*, 43, 2795–2800.

Pinto, I., Pereira, H., and Usenius, A., 2004. Heartwood and sapwood development within maritime pine (Pinus pinaster Ait.) stems. *Trees*, 18, 284–294.

Ray, U., *et al.*, 2021. Mechanics design in cellulose-enabled high-performance functional materials. *Advanced Materials*, 33, 2002504.

Schwarze, F.W.M.R., 2007. Wood decay under the microscope. *Fungal Biology Reviews*, 21, 133–170.

Sivan, P., Rao, K.S., and Rajput, K.S., 2023. Chemical composition in juvenile and mature wood of branch and main trunk of leucaena leucocephala (Lam.) de Wit. *Plants*, 12 (23), 3977.

Smith, P.M., and Wolcott, M.P., 2006. Opportunities for wood/natural fiber-plastic composites in residential and industrial applications. *Forest Products Journal*, 56 (3), 4–11.

Sukiman, M.S., et al., 2020. Design and numerical modeling of the thermoforming process of a WPC based formwork structure. *Materials Today Communications*, 22, 100805.

Tazi, M., *et al.*, 2014. Characterization of rheological and thermophysical properties of HDPE–wood composite. *Journal of Applied Polymer Science*, 131 (13), 40495.

Tazi, M., Erchiqui, F., and Kaddami, H., 2016. Influence of SOFTWOOD-fillers content on the biodegradability and morphological properties of WOOD–polyethylene composites. *Polymer Composites*, 39, 29–37.

Ten, E., and Vermerris, W., 2015. Recent developments in polymers derived from industrial lignin. *Journal of Applied Polymer Science*, 132 (24), 42069.

Ten Have, R., and Teunissen, P.J.M., 2001. Oxidative mechanisms involved in lignin degradation by white-rot fungi. *Chemical Reviews*, 101, 3397–3414.

Via, B.K., *et al.*, 2007. Within tree variation of lignin, extractives, and microfibril angle coupled with the theoretical and near infrared modeling of microfibril angle. *Iawa Journal*, 28, 189–210.

Via, B.K., *et al.*, 2009. Mechanical response of longleaf pine to variation in microfibril angle, chemistry associated wavelengths, density, and radial position. *Composites Part A: Applied Science and Manufacturing*, 40, 60–66.

Wang, W., *et al.*, 2020. Mechanical and thermal behavior analysis of wood–polypropylene composites. *Textile Research Journal*, 91, 347–357.

Zhang, K., *et al.*, 2023. Ambient-densified and polymer-free transparent wood film for smart food packaging window. *iScience*, 26, 108455.

Zobel, B., and Blair, R., 1976. Wood and pulp properties of juvenile wood and topwood of the southern pines. *Applied Polymer Symposium*, 28, 421–433.